Journal of Magnetic Resonance **139,** 132–138 (1999)
Article ID jmre.1999.1761, available online at http://www.idealibrary.com on IDEAL®

Calculation of MAS Spectra Influenced by Slow Molecular Tumbling

C. Mayer

Institut für Physikalische und Theoretische Chemie, Universität Duisburg, 47048 Duisburg, Germany

Received December 14, 1998; revised March 17, 1999

A numeric algorithm is proposed that is suitable to calculate spectral lineshapes influenced by isotropic and anisotropic tumbling under sample spinning conditions. It is based on the stochastic Liouville equation and a rotational diffusion process described by a stationary Markov operator. A corresponding FORTRAN program can be implemented on a regular personal computer. The calculations result in spectral lineshapes including a complete set of spinning sidebands. The sensitive time scale of the resulting lineshapes depends on the deviation of the sample spinning axis from the magic angle. An example is presented demonstrating the potential of off-magic-angle spinning as a tool to analyze slow tumbling motions. © 1999 Academic Press

INTRODUCTION

The application of sample spinning in magnetic resonance spectroscopy offers a variety of advantages that have led to its extensive use in the past (*1–5*). The gain in signal-to-noise ratio and the possibility to avoid overlap between adjacent signals may be the most important improvements achieved by this procedure. In addition, the technique may be used to determine the elements of a chemical shift tensor (*6–8*).

However, the method of sample spinning also complicates the analysis of NMR spectra, especially when it comes to analyzing slow motions. A number of approaches have been developed to simulate magic angle spinning (MAS) spectra on the basis of jump motions between two or three sites (*5, 9–12*) or in cases where no motionally induced relaxation is present (*13–16*), but so far, to the knowledge of the author, no attempt has been made to describe diffusive motion in connection with sample spinning.

In the following, a numeric algorithm is proposed to permit one to calculate spectra based on molecular tumbling in the presence of anisotropic chemical shift under sample spinning conditions. The procedure is based on the introduction of small steps in three Euler angle domains and in time, similar to an algorithm proposed for static spectra that has been described before (*17*). The simulated spectra exhibit rotational sidebands with relative intensities that are in accordance with results derived from analytical determinations (*6*). As expected, molecular tumbling strongly affects the efficiency of MAS and may lead to a significant line broadening, the linewidth being a function of motional correlation times. Finally, it is shown how a small deviation from the magic angle may be used to increase the significance of variations of the spectral lineshapes with the tumbling rate.

THEORETICAL CONSIDERATIONS

Numerical Calculation of NMR Spectra

The time-dependent ensemble average magnetization of any spin system can be conveniently described by the density operator $\rho(t)$ (*18, 19*). In the presence of a time-independent Hamilton operator and disregarding any other source of relaxation, it develops according to

$$\frac{\partial}{\partial t}\rho(t) = -i/\hbar[H, \rho(t)]. \qquad [1]$$

Under static conditions (no MAS), the Hamiltonian depends on the molecular orientation with respect to a given sample container, marked by a set of Euler angles Ω_n. This leads to an angular dependence of ρ and H. With sample spinning, the Hamiltonian for each molecular orientation Ω_n also becomes time dependent. Therefore, Eq. [1] converts to

$$\frac{\partial}{\partial t}\rho(\Omega_n, t) = -i/\hbar[H(\Omega_n, t), \rho(\Omega_n, t)]. \qquad [2]$$

Moreover, motional processes in a discretized diffusion sphere lead to an exchange of magnetization between the orientations Ω_n described by a set of rate constants $k_{(\Omega n \to \Omega n')}$ (*17*):

$$\frac{\partial}{\partial t}\rho(\Omega_n, t) = -i/\hbar[H(\Omega_n, t), \rho(\Omega_n, t)] + \sum_{n'}\{-k_{(\Omega n \to \Omega n')}[\rho(\Omega_n, t) - \rho^{eq}(\Omega_n)] + k_{(\Omega n' \to \Omega n)}[\rho(\Omega_{n'}, t) - \rho^{eq}(\Omega_{n'})]\}. \qquad [3]$$

The time dependence of the density matrix elements for all orientations Ω_n is thus completely described by a set of coupled differential equations. The actual signal contribution for

1090-7807/99 $30.00

each orientation Ω_n in the rotating frame is then given by $M(\Omega_n, t) \propto \mathrm{Tr}[\rho(\Omega_n, t)I^+]$. We now introduce short time intervals Δt as an equivalent to the experimental dwell time. Within such a (sufficiently short) time interval, the effect of motion may be separated from the effect of Larmor precession. Based on this approximation, the signal contribution $M(\Omega_n, t + \Delta t)$ is derived from $M(\Omega_n, t)$ by (*17*)

$$M(\Omega_n, t + \Delta t) = M(\Omega_n, t)\exp(i\omega(\Omega_n, t)\Delta t) + \sum_{n'} [-k_{(\Omega n \to \Omega n')}\Delta t M(\Omega_n, t)\exp(i\omega(\Omega_n, t)\Delta t) + k_{(\Omega n' \to \Omega n)}\Delta t M(\Omega_{n'}, t)\exp(i\omega(\Omega_{n'}, t)\Delta t)]. \quad [4]$$

With the initial values of $M(\Omega_n, 0)$ set to the equilibrium populations of the sites in molecular orientation Ω_n,

$$M(\Omega_n, 0) = P_{\mathrm{eq}}(\Omega_n), \quad [5]$$

and the overall value of the detectable free induction decay given by

$$M_{\mathrm{tot}}(t) = \sum_n M(\Omega_n, t), \quad [6]$$

Eq. [4] describes the time-dependent variation of an NMR signal after a $\pi/2$-pulse. Accordingly, the free induction decay (FID) can be numerically calculated in an iterative procedure (*17*) until its absolute value decreases to less than one thousandth of the original intensity. At any time during the evolution of the FID, the effect of a π-pulse may be simulated by simply inverting the real or the imaginary part of all contributions $M(\Omega_n, t)$ (*17*). The desired spectral lineshape is finally obtained by Fourier transformation.

In order to derive MAS spectra in the presence of rotational diffusion according to Eqs. [4] to [6], it is necessary to define appropriate expressions (a) for the orientation and, because of sample spinning, time-dependent Larmor frequencies $\omega(\Omega_n, t)$ for each site Ω_n, and (b) for the rate constants $k_{(\Omega n \to \Omega n')}$. These will be derived in the next sections.

Orientation and Time Dependence of the Larmor Frequency $\omega(\Omega_n, t)$

The basic set of coordinate systems necessary to describe the effect of sample rotation in the presence of rotational diffusion is given in Fig. 1. In the most general case, four systems of reference are required. However, for isotropic tumbling, the minimum number of systems is reduced to three. All examples illustrated in the following sections are calculated for isotropic rotational diffusion.

(a) Magnetic tensor system. The magnetic tensor system is defined by the orientation of the interaction tensor, e.g., the Hamiltonian for chemical shift anisotropy $H_{\mathrm{CS}} = \gamma\hbar I\sigma B$. Within this reference frame, only diagonal elements of the shielding tensor σ_{xx}, σ_{yy}, σ_{zz} exist. For ^{13}C-nuclei in a number of representative molecules, actual values for σ_{xx}, σ_{yy}, and σ_{zz} have been determined applying various experimental techniques (*20*). Correspondingly, the chemical shift anisotropy tensor in the magnetic tensor system is given by

$$\sigma^{\mathrm{M}} = \begin{pmatrix} \sigma_{xx} & 0 & 0 \\ 0 & \sigma_{yy} & 0 \\ 0 & 0 & \sigma_{zz} \end{pmatrix}. \quad [7]$$

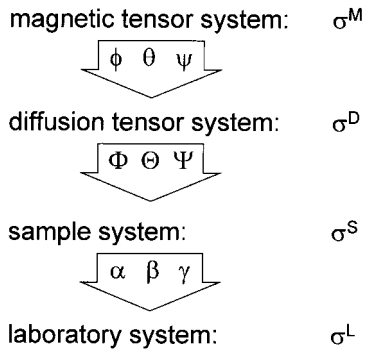

FIG. 1. Set of coordinate systems and Euler transformation angles required for a general description of anisotropic diffusion under sample spinning conditions. In the magnetic tensor system, the interaction tensor matrix (for example, σ^{M}) consists of diagonal elements only. The axes of the diffusion tensor system coincide with the long and the two short rotation axes of the molecule. The z-axis of the sample system is identical with the rotation axis of the rotor; the z-axis of the laboratory system is defined by the direction of the external magnetic field. The diffusive motion of the molecules is characterized by jump motions between sites in Φ, Θ, and Ψ; the sample rotation is described by $\alpha(t)$ and a tilt angle β. In the case of isotropic rotation, the result does not depend on ϕ, θ, and ψ (which therefore are set to zero for the examples in the text).

(b) Diffusion tensor system. This reference frame is determined by the symmetry and the shape of the molecule. It coincides with the long and two short axes of a hypothetical ellipsoid that most closely resembles the averaged molecular geometry. The expression for the chemical shift tensor in the diffusion tensor system σ^{D} results from σ^{M} by application of a corresponding Euler transformation (*21*):

$$\sigma^{\mathrm{D}} = T^{\mathrm{MD}}\sigma^{\mathrm{M}}T^{\mathrm{MD}-1}. \quad [8]$$

In the case of isotropic rotation, the diffusion tensor system can be chosen to be identical to the magnetic tensor system ($\sigma^{\mathrm{D}} = \sigma^{\mathrm{M}}$).

(c) Sample system. The sample system is defined by the geometry of the sample container, e.g., the rotor of the actual MAS experiment, the z_s-axis coinciding with its symmetry

(rotation) axis. Again, the corresponding chemical shift tensor is obtained by a Euler transformation (*21*):

$$\sigma^{S} = T^{DS}(\Phi_k, \Theta_l, \Psi_m)\sigma^{D}T^{DS-1}(\Phi_k, \Theta_l, \Psi_m). \quad [9]$$

The Euler angles Φ_k, Θ_l, and Ψ_m describe the orientation Ω of the molecule with respect to the MAS rotor.

(d) Laboratory system. The laboratory system is determined by the orientation of the NMR magnet, its *z*-axis describing the orientation of the magnetic field. Here, the relevant chemical shift tensor is derived as

$$\sigma^{L} = T^{SL}(\alpha, \beta, \gamma)\sigma^{S}T^{SL-1}(\alpha, \beta, \gamma). \quad [10]$$

Because of the axial symmetry of the magnetic field, the result does not depend on the Euler angle γ, which therefore can be set to zero. The angle β describes the orientation of the rotation axis versus the magnetic field (e.g., 54.7° in the case of MAS), while α is time dependent with the frequency of sample rotation ω_r according to

$$\alpha(t) = \omega_r t. \quad [11]$$

With the Euler transformations given above, the chemical shift tensor in the laboratory system is represented by

$$\sigma^{L} = T^{SL}(\alpha(t), \beta, 0)\sigma^{S}T^{SL-1}(\alpha(t), \beta, 0). \quad [12]$$

With

$$T^{SL} = \begin{pmatrix} \cos\beta\cos\alpha & \cos\beta\sin\alpha & -\sin\beta \\ -\sin\alpha & \cos\alpha & 0 \\ \sin\beta\cos\alpha & \sin\beta\sin\alpha & \cos\beta \end{pmatrix} \quad [13]$$

and

$$T^{SL-1} = \begin{pmatrix} \cos\beta\cos\alpha & -\sin\alpha & \sin\beta\cos\alpha \\ \cos\beta\sin\alpha & \cos\alpha & \sin\beta\sin\alpha \\ -\sin\beta & 0 & \cos\beta \end{pmatrix}, \quad [14]$$

the relevant *zz*-element of this tensor results in

$$\begin{aligned}\sigma^{L}_{zz} = {} & \sin\beta\cos\alpha(\sin\beta\cos\alpha\sigma^{S}_{xx} + \sin\beta\sin\alpha\sigma^{S}_{xy} \\ & + \cos\beta\sigma^{S}_{xz}) + \sin\beta\sin\alpha(\sin\beta\cos\alpha\sigma^{S}_{yx} \\ & + \sin\beta\sin\alpha\sigma^{S}_{yy} + \cos\beta\sigma^{S}_{yz}) \\ & + \cos\beta(\sin\beta\cos\alpha\sigma^{S}_{zx} \\ & + \sin\beta\sin\alpha\sigma^{S}_{zy} + \cos\beta\sigma^{S}_{zz}). \end{aligned} \quad [15]$$

This value is identical with the orientation and time-dependent Larmor frequency in the rotating frame $\omega(\Omega_n, t)$, the final result therefore becomes

$$\begin{aligned}\sigma^{L}_{zz}(\Omega_n, t) &= \sigma^{L}_{zz}(\Phi_k, \Theta_l, \Psi_m, t) \\ &= [\cos^2\beta\sigma^{S}_{zz}] + \sin^2(\omega_r t)[\sin^2\beta\sigma^{S}_{yy}] \\ &\quad + \cos^2(\omega_r t)[\sin^2\beta\sigma^{S}_{xx}] + \sin(\omega_r t)\cos(\omega_r t) \\ &\quad \times [\sin^2\beta(\sigma^{S}_{xy} + \sigma^{S}_{yx})] \\ &\quad + \sin(\omega_r t)[\sin\beta\cos\beta(\sigma^{S}_{yz} + \sigma^{S}_{zy})] \\ &\quad + \cos(\omega_r t)[\sin\beta\cos\beta(\sigma^{S}_{xz} + \sigma^{S}_{zx})], \end{aligned} \quad [16]$$

with the elements of σ^{S} given by

$$\sigma^{S} = T^{DS}(\Phi_k, \Theta_l, \Psi_m)\sigma^{D}T^{DS-1}(\Phi_k, \Theta_l, \Psi_m). \quad [17]$$

With $\omega(\Omega_n, t) = \omega_0\sigma^{L}_{zz}(\Omega_n, t)$ and by combining Eqs. [16] and [17], an expression for the time-dependent Larmor frequency in the rotating frame can be derived for any given molecular orientation Ω_n (specified by Φ_k, Θ_l, and Ψ_m) in the sample system.

Motionally Induced Exchange Processes $k_{(\Omega n \rightarrow \Omega n')}$

It is assumed that rotational diffusion leads to a continuous exchange of individual molecules between the given orientations Ω_n. Generally, the motion of an ellipsoid in a viscous medium is described by two correlation times $\tau_\parallel$ and $\tau_\perp$, referring to rotational diffusion along the long axis and the two short axes, respectively. Based on relative populations $P_{rel} = (P/P_{eq})$ of orientations given by Euler angles Φ, Θ, and Ψ, the corresponding diffusion operator can be formulated as (*22*, *23*)

$$\Gamma_{dif}P_{rel} = \frac{\partial P_{rel}}{\partial t} \quad [18]$$

$$\begin{aligned}\Gamma_{dif} = {} & \frac{1}{6\tau_\parallel}\frac{\partial^2}{\partial\Phi^2} + \frac{1}{6\tau_\perp}\left(\frac{\partial^2}{\partial\Theta^2} + \cot^2\Theta\frac{\partial^2}{\partial\Phi^2} + \frac{1}{\sin^2\Theta}\frac{\partial^2}{\Psi^2}\right. \\ & \left. - 2\frac{\cot\Theta}{\sin\Theta}\frac{\partial^2}{\partial\Phi\partial\Psi} + \cot\Theta\frac{\partial}{\partial\Theta}\right), \end{aligned} \quad [19]$$

which may be separated into its angular contributions:

$$\Gamma_\Phi = \frac{1}{6\tau_\parallel}\frac{\partial^2}{\partial\Phi^2} + \frac{1}{6\tau_\perp}\cot^2\Theta\frac{\partial^2}{\partial\Phi^2} \quad [20]$$

$$\Gamma_\Theta = \frac{1}{6\tau_\perp}\frac{\partial^2}{\partial\Theta^2} + \frac{1}{6\tau_\perp}\cot\Theta\frac{\partial}{\partial\Theta} \quad [21]$$

$$\Gamma_\Psi = \frac{1}{6\tau_\perp}\frac{1}{\sin^2\Theta}\frac{\partial^2}{\partial\Psi^2} \quad [22]$$

$$\Gamma_{\Phi\Psi} = \frac{1}{6\tau_\perp}\left(-2\frac{\cot\Theta}{\sin\Theta}\frac{\partial^2}{\partial\Phi\partial\Psi}\right). \quad [23]$$

The described relaxation model requires the segmentation of the diffusion sphere. This results in the definition of discrete angular sites Ω_n specified by sets of Euler angles Φ_k, Θ_l, and Ψ_m. With

$$\begin{aligned} &n_\Phi \text{ sites between } \Phi_{\min} = 0 \text{ and } \Phi_{\max} = 2\pi \\ &\qquad (\text{and } \Delta\Phi = 2\pi/n_\Phi) \\ &n_\Theta \text{ sites between } \Theta_{\min} = 0 \text{ and } \Theta_{\max} = \pi \\ &\qquad (\text{and } \Delta\Theta = \pi/n_\Theta) \\ &n_\Psi \text{ sites between } \Psi_{\min} = 0 \text{ and } \Psi_{\max} = 2\pi \\ &\qquad (\text{and } \Delta\Psi = 2\pi/n_\Psi), \end{aligned}$$

an overall number of $n = n_\Phi n_\Theta n_\Psi$ discrete orientations Ω_n is obtained. Consequently, the diffusion operator Γ now yields a set of rate constants describing the exchange rates between adjacent sites differing in one or two Euler angles:

$$\begin{aligned} k(\Phi_k \rightarrow \Phi_{k+1}) &= k(\Phi_k \rightarrow \Phi_{k-1}) \\ &= \left(\frac{1}{6\tau_\parallel} + \frac{1}{6\tau_\perp}\cot^2\Theta\right)\frac{1}{(\Delta\Phi)^2} \qquad [24] \end{aligned}$$

$$k(\Theta_l \rightarrow \Theta_{l\pm1}) = \frac{1}{6\tau_\perp}\frac{\sqrt{\sin\Theta_{l\pm1}}}{\sqrt{\sin\Theta_l}}\frac{1}{(\Delta\Theta)^2} \qquad [25]$$

$$\begin{aligned} k(\Psi_m \rightarrow \Psi_{m+1}) &= k(\Psi_m \rightarrow \Psi_{m-1}) \qquad [26] \\ &= \frac{1}{6\tau_\perp}\frac{1}{\sin^2\Theta}\frac{1}{(\Delta\Psi)^2} \end{aligned}$$

$$\begin{aligned} k\begin{pmatrix}\Phi_k \rightarrow \Phi_{k+1}\\ \Psi_m \rightarrow \Psi_{m+1}\end{pmatrix} &= k\begin{pmatrix}\Phi_k \rightarrow \Phi_{k-1}\\ \Psi_m \rightarrow \Psi_{m-1}\end{pmatrix} \\ &= -\frac{1}{6\tau_\perp}2\frac{\cot\Theta}{\sin\Theta}\frac{1}{4(\Delta\Phi)(\Delta\Psi)} \qquad [27] \end{aligned}$$

$$\begin{aligned} k\begin{pmatrix}\Phi_k \rightarrow \Phi_{k+1}\\ \Psi_m \rightarrow \Psi_{m-1}\end{pmatrix} &= k\begin{pmatrix}\Phi_k \rightarrow \Phi_{k-1}\\ \Psi_m \rightarrow \Psi_{m+1}\end{pmatrix} \\ &= \frac{1}{6\tau_\perp}2\frac{\cot\Theta}{\sin\Theta}\frac{1}{4(\Delta\Phi)(\Delta\Psi)}. \qquad [28] \end{aligned}$$

With the corresponding normalized distribution function, which in the absence of an orienting potential becomes

$$P_{\text{eq}}(\Omega_n) = P_{\text{eq}}(\Phi_k\Theta_l\Psi_m) = \frac{\sin\Theta_l}{n_\Phi n_\Psi \sum_{l'}\sin\Theta_{l'}} = \frac{\sin\Theta_l}{c}, \qquad [29]$$

the expressions for the rate constants automatically fulfill the condition for detailed balance:

$$P_{\text{eq}}(\Omega_n)k_{(\Omega n\rightarrow\Omega n')} = P_{\text{eq}}(\Omega_{n'})k_{(\Omega n'\rightarrow\Omega n)}. \qquad [30]$$

Any deviation from the equilibrium populations leads to a net change of site populations with time determined by the rate constants. For an infinite number of sites, the time dependence $\partial P(\Omega_n)/\partial t$ derived from first-order kinetics is equivalent to the expression given by the diffusion operator. This is done to justify the expressions [24] to [28], as may be shown in the following for the example of $k(\Theta_l \rightarrow \Theta_{l'})$.

Consider three adjacent sites 1, 2, and 3 with Θ_1, Θ_2, and Θ_3. Then the time dependence of the absolute population of site 2 is given by

$$\begin{aligned} \frac{dP_2}{dt} &= k_{(\Theta_1\rightarrow\Theta_2)}P_1 - k_{(\Theta_2\rightarrow\Theta_1)}P_2 \\ &\quad + k_{(\Theta_3\rightarrow\Theta_2)}P_3 - k_{(\Theta_2\rightarrow\Theta_3)}P_2, \qquad [31] \end{aligned}$$

which according to Eq. [25] yields

$$\begin{aligned} \frac{dP_2}{dt} = \frac{1}{6\tau_\perp}\frac{1}{(\Delta\Theta)^2}\Bigg(&\frac{\sqrt{\sin\Theta_2}}{\sqrt{\sin\Theta_1}}P_1 - \frac{\sqrt{\sin\Theta_1}}{\sqrt{\sin\Theta_2}}P_2 \\ &+ \frac{\sqrt{\sin\Theta_2}}{\sqrt{\sin\Theta_3}}P_3 - \frac{\sqrt{\sin\Theta_3}}{\sqrt{\sin\Theta_2}}P_2\Bigg), \qquad [32] \end{aligned}$$

and, with $P = P_{\text{rel}}P_{\text{eq}}$ and Eq. [29]:

$$\begin{aligned} \frac{dP_2}{dt} &= \frac{1}{c6\tau_\perp}\frac{1}{(\Delta\Theta)^2}(\sin\Theta_{12}P_{1\text{rel}} - \sin\Theta_{12}P_{2\text{rel}} \\ &\quad + \sin\Theta_{23}P_{3\text{rel}} - \sin\Theta_{23}P_{2\text{rel}}), \qquad [33] \end{aligned}$$

where $\sin\Theta_{nm}$ stands for $\sqrt{\sin\Theta_n\sin\Theta_m}$. Rearrangement of Eq. [33] yields

$$\begin{aligned} \frac{dP_2}{dt} &= \frac{1}{c6\tau_\perp}\frac{1}{(\Delta\Theta)^2}[\sin\Theta_{23}(P_{3\text{rel}} - P_{2\text{rel}}) \\ &\quad - \sin\Theta_{12}(P_{2\text{rel}} - P_{1\text{rel}})] \\ &= \frac{1}{c6\tau_\perp}\frac{1}{\Delta\Theta}\left[\sin\Theta_{23}\left(\frac{P_{3\text{rel}} - P_{2\text{rel}}}{\Delta\Theta}\right)\right. \\ &\quad \left. - \sin\Theta_{12}\left(\frac{P_{2\text{rel}} - P_{1\text{rel}}}{\Delta\Theta}\right)\right]. \qquad [34] \end{aligned}$$

With infinitesimally small angular steps $\Delta\Theta$, Eq. [34] may be brought into a differential form:

$$\frac{dP_2}{dt} = \frac{1}{c6\tau_\perp}\frac{\partial}{\partial\Theta}\left[\sin\Theta\left(\frac{\partial P}{\partial\Theta}\right)\right]$$

$$= \frac{1}{c6\tau_\perp}\left[\sin\Theta\left(\frac{\partial^2 P}{\partial\Theta^2}\right) + \cos\Theta\left(\frac{\partial P}{\partial\Theta}\right)\right] \quad [35]$$

$$\frac{dP_{2\mathrm{rel}}}{dt} = \frac{1}{\sin\Theta 6\tau_\perp}\left[\sin\Theta\left(\frac{\partial^2 P}{\partial\Theta^2}\right) + \cos\Theta\left(\frac{\partial P}{\partial\Theta}\right)\right]$$

$$= \frac{1}{6\tau_\perp}\left(\frac{\partial^2 P}{\partial\Theta^2}\right) + \frac{1}{6\tau_\perp}\cot\Theta\left(\frac{\partial P}{\partial\Theta}\right). \quad [36]$$

The last expression is essentially identical to Eq. [21]. Similarly, the procedure described above can be reproduced for the other rate constants to prove their validity.

GENERAL PROCEDURE

All computations were performed on a regular personal computer applying a FORTRAN program based on the described formalism. Alternatively, the algorithm can be implemented on common spreadsheet software, as described before for the calculation of static NMR spectra (*17*). However, because of the necessity of an additional angular sphere for the simulation of MAS spectra, the spreadsheet approach suffers from serious storage limitations and therefore remains restricted to simple problems.

An important requirement for reliable results is a suitable selection of values for the four key parameters of the numeric calculation: the numbers of sites n_Φ, n_Θ, and n_Ψ for the three angular domains, and the length of the time interval Δt in the time regime. As a first condition, the site number should be large enough to avoid visible gaps between the angular contributions to the spectral lineshape. Very slow molecular tumbling with correlation times larger than the reciprocal chemical shift anisotropy typically requires site numbers of $n_\Phi = n_\Theta = n_\Psi > 40$. As a second condition, the time interval Δt has to be chosen short enough to allow the approximation described by Eq. [4]. As a rule of thumb, not more than 10% of the given magnetization of any site should be transferred in the course of each time interval. In any case, as a final verification of the result, the spectral lineshape should be checked for convergence with increasing site numbers and decreasing Δt. Computation times depend strongly on the specific problem. They vary between 5 min for spectra based on rapid tumbling and 12 h for slow motional lineshapes with correspondingly large site numbers. All results given in the next section were obtained within less than 3 h per spectrum.

If the diffusive motion is either extremely rapid or extremely slow, the described algorithm becomes inefficient because of the resulting long relaxation period. In this case, an alternative approach, which limits the simulation to a single period of the MAS experiment and neglects relaxation due to molecular motion (or replaces it by a phenomenological term), is strongly recommended (*13–15*). For additional convenience, it may be combined with a simplified powder averaging procedure (*14–16*).

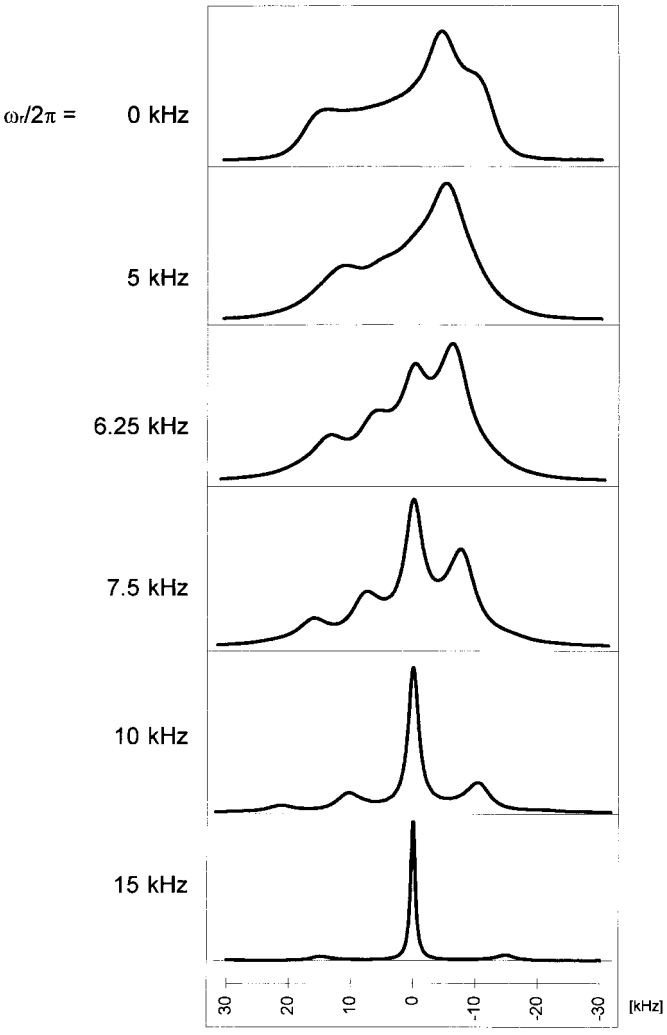

FIG. 2. Calculated MAS spectra obtained under variation of the spinning frequency. The interaction tensor is assumed to represent chemical shift anisotropy with tensor elements $\sigma_{xx} = -15$ kHz, $\sigma_{yy} = -5$ kHz, and $\sigma_{zz} = 20$ kHz. The molecular motion responsible for a significant distortion of the original powder pattern is a simulated isotropic tumbling with $\tau_\parallel = \tau_\perp = 0.1$ ms, which is approximated by jump processes between 13*13*13 sites for the three angular domains. The original FIDs where obtained in 80,000 time intervals of 30 ns duration. All spectra are normalized to identical areas; the intensity axis is suitably expanded.

REPRESENTATIVE RESULTS

Effect of Rotation Frequency

An example of calculated MAS spectra obtained under variation of the spinning frequency is shown in Fig. 2. The inter-

action tensor is assumed to represent chemical shift anisotropy with tensor elements $\sigma_{xx} = -15$ kHz, $\sigma_{yy} = -5$ kHz, and $\sigma_{zz} = 20$ kHz. The molecular motion responsible for a significant distortion of the original powder pattern (see Fig. 2 at $\omega_r/2\pi = 0$ kHz) is a simulated isotropic tumbling with $\tau_\parallel = \tau_\perp = 0.1$ ms. With 13*13*13 sites and 80,000 time intervals ($\Delta t = 30$ ns) for the complete FID, the computation time was in the range of 25 min. All spectra are normalized; the intensity axis is suitably expanded.

As expected, the static spectrum ($\omega_r/2\pi = 0$ kHz) exhibits the well-known features of a powder pattern slightly affected by isotropic diffusion. With increasing frequency of sample spinning, the rotational sidebands appear, move away from the zero frequency, and lose intensity to the centerband.

Variation of Tumbling Rate

The effect of various correlation times on calculated MAS spectra is shown in Fig. 3. The tensor elements are the same as before; the spinning frequency is set to $\omega_r/2\pi = 10$ kHz. Correlation times of isotropic tumbling ($\tau_\parallel$ and $\tau_\perp$) are varied between 0.01 and 1 ms. Again, site numbers for the angular domains were set to 13*13*13.

Only for the largest value ($\tau_\parallel = \tau_\perp = 1$ ms) do the centerband and all sidebands appear to be well separated. Their relative intensities $I_{20\text{kHz}}/I_0 = 0.107$, $I_{10\text{kHz}}/I_0 = 0.274$, $I_{-10\text{kHz}}/I_0 = 0.420$, and $I_{-20\text{kHz}}/I_0 = 0.049$ are in good accordance with values determined by the procedure of Herzfeld and Berger (*6*), which yields $I_{20\text{kHz}}/I_0 = 0.113$, $I_{10\text{kHz}}/I_0 = 0.279$, $I_{-10\text{kHz}}/I_0 = 0.426$, and $I_{-20\text{kHz}}/I_0 = 0.053$. Following the proposition by Maricq and Waugh (*5*), the linewidth of the centerband can be used to determine the correlation time of the isotropic diffusion, as its dependence on the tumbling rate is significant within the given time scale.

Simulated Off-Angle Spinning

In most cases, spectroscopists deal with numerous potential sources of linewidth variation. Typical examples may be incomplete suppression of dipolar coupling and conformational isomerization. Therefore, it is desirable to create experimental conditions that lead to spectral features that reflect motional parameters more significantly than just the linewidth. One possibility is to apply sample rotation at an offset to the magic angle (see, for example, *24–27*). A small offset results in spectra with centerbands roughly resembling the lineshapes obtained under static conditions. However, as the overall linewidth is significantly reduced, they still offer the advantages of improved signal-to-noise ratio and reduced overlap of adjacent signals.

Figure 4 shows calculated results based on parameters given before ($\sigma_{xx} = -15$ kHz, $\sigma_{yy} = -5$ kHz, and $\sigma_{zz} = 20$ kHz, $\omega_r/2\pi = 10$ kHz), but with a rotation angle of $\beta = 50°$ instead of 54.7° and for correlation times $\tau = \tau_\parallel = \tau_\perp$ of 0.3 to 10 ms. The site numbers vary from 17*17*17 to 27*27*27 and com-

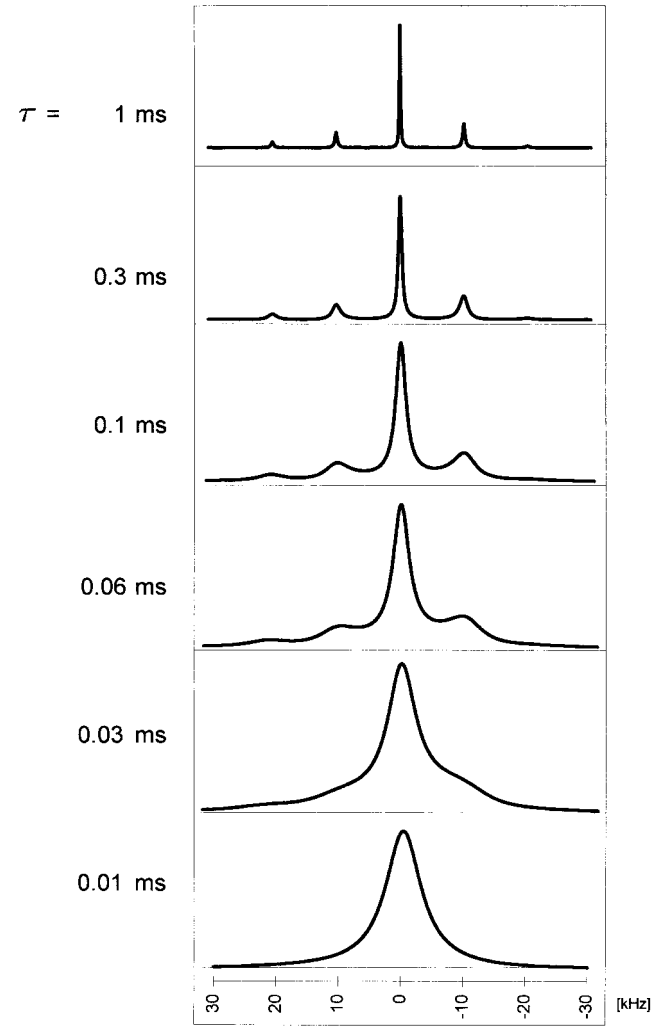

FIG. 3. Simulated MAS spectra obtained under variation of the tumbling rate. Again, the interaction tensor is assumed to represent chemical shift anisotropy with tensor elements $\sigma_{xx} = -15$ kHz, $\sigma_{yy} = -5$ kHz, and $\sigma_{zz} = 20$ kHz. The spinning frequency is set to $\omega_r/2\pi = 10$ kHz. Correlation times of isotropic tumbling ($\tau = \tau_\parallel = \tau_\perp$) are varied between 0.01 and 1 ms; the motion is approximated in 13*13*13 sites for the three angular domains. The spectra are derived from FIDs calculated in 80,000 steps of 30 ns duration.

putation times from 1 h to almost 3 h depending on the tumbling rate. The second left sideband, the centerband, and the second right sideband of each resulting spectrum are displayed separately; both sidebands are magnified by a factor of 10 for better resolution.

In this case, the spectra not only differ in the linewidth of the signal, but also show significant variation in characteristic features. The lineshape of the centerband deviates strongly from the lineshapes of the sidebands, which is explained by an angular dependence of the sideband intensities. A comparison with Fig. 3 also shows that the sensitive time scale has shifted toward slower motions. This indicates the partial averaging of

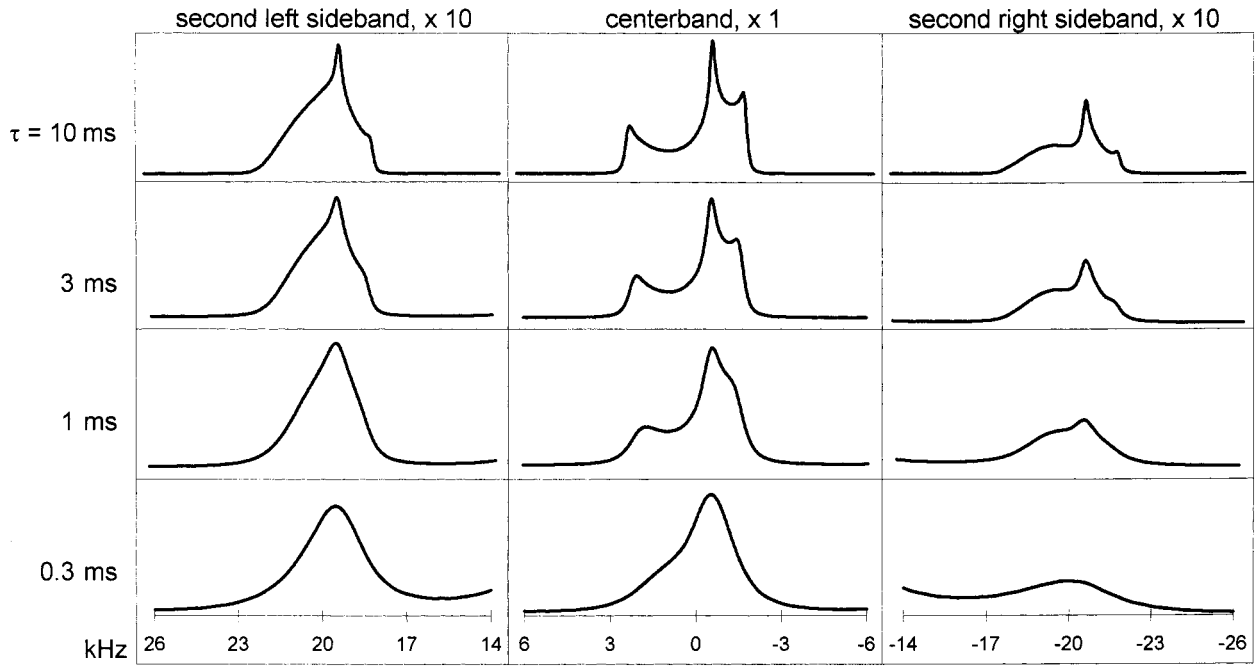

FIG. 4. Simulated spectra for sample spinning at a tilt angle of $\beta = 50°$ for various tumbling rates between 0.3 and 10 ms. The second left sideband, the centerband, and the second right sideband of each resulting spectrum are shown separately to improve resolution; the sidebands are magnified by a factor of 10. Simulation parameters are as in Figs. 2 and 3 ($\sigma_{xx} = -15$ kHz, $\sigma_{yy} = -5$ kHz, and $\sigma_{zz} = 20$ kHz, $\omega_r/2\pi = 10$ kHz), except for the rotation angle (50° instead of 54.7°), correlation times ($\tau = \tau_{\parallel} = \tau_{\perp}$ vary from 0.3 to 10 ms), and site numbers (see text).

the tensor by sample rotation and may be used to vary the dynamic range of the experiment.

CONCLUSION

The described approach allows numerical calculation of spectral lineshapes based on isotropic and anisotropic tumbling under sample spinning conditions. Implemented in a FORTRAN program or even, for simple cases, as a spreadsheet, it can be run on any regular personal computer. Additional experimental or sample conditions such as π-pulses, orienting potentials, or any deviation from the magic angle are easily introduced. Off-magic-angle spinning presents a promising experimental approach to maximize the sensitivity of spectral lineshapes toward variations of the tumbling rates.

REFERENCES

1. I. Lowe, *Phys. Rev. Lett.* **2,** 285 (1959).
2. E. R. Andrew, A. Bradbury, and R. G. Eades, *Nature* **182,** 1659 (1958).
3. E. R. Andrew, A. Bradbury, and R. G. Eades, *Nature* **183,** 1802 (1959).
4. J. Schaefer and E. O. Stejskal, *J. Am. Chem. Soc.* **98,** 1031 (1976).
5. M. Matti Maricq and J. S. Waugh, *J. Chem. Phys.* **70,** 3300 (1979).
6. J. Herzfeld and A. E. Berger, *J. Chem. Phys.* **73,** 6021 (1980).
7. M. G. Munowitz, R. G. Griffin, G. Bodenhausen, and T. C. Huang, *J. Am. Chem. Soc.* **103,** 2529 (1981).
8. W. Gabrielse, H. F. J. M. van Well, and W. S. Veeman, *Solid State Nucl. Magn. Reson.* **6,** 231 (1996).
9. A. Schmidt, S. O. Smith, D. P. Raleigh, J. E. Roberts, R. G. Griffin, and S. Vega, *J. Chem. Phys.* **85,** 4248 (1986).
10. A. Schmidt and S. Vega, *J. Chem. Phys.* **87,** 6895 (1987).
11. A. C. Kolbert, D. P. Raleigh, and R. G. Griffin, *J. Magn. Reson.* **82,** 483 (1989).
12. J. R. Long, B. Q. Sun, A. Bowen, and R. G. Griffin, *J. Am. Chem. Soc.* **116,** 11950 (1994).
13. M. Edén, Y. K. Lee, and M. H. Levitt, *J. Magn. Reson. A* **120,** 56 (1996).
14. M. H. Levitt and M. Eden, *Mol. Phys.* **95,** 879 (1998).
15. T. Charpentier, C. Fermon, and J. Virlet, *J. Magn. Reson.* **132,** 181 (1998).
16. T. Charpentier, C. Fermon, and J. Virlet, *J. Chem. Phys.* **109,** 3116 (1998).
17. C. Mayer, *J. Magn. Reson.,* in press.
18. A. Abragam, "The Principles of Nuclear Magnetism," Oxford Univ. Press, London (1961).
19. C. P. Slichter, "Principles of Magnetic Resonance," Springer, Berlin (1978).
20. W. S. Veeman, *Prog. Nucl. Magn. Reson. Spectrosc.* **16,** 193 (1984).
21. S. P. Van, G. B. Birrell, and O. H. Griffith, *J. Magn. Reson.* **15,** 444 (1974).
22. F. Perrin, *J. Phys. Radium* **5,** 497 (1934).
23. F. Perrin, *J. Phys. Radium* **7,** 1 (1936).
24. A. C. Kolbert, P. J. Grandinetti, M. Baldwin, S. B. Prusiner, and A. Pines, *J. Phys. Chem.* **98,** 7936 (1994).
25. S. Ding and C. A. McDowell, *J. Magn. Reson.* **117,** 171 (1995).
26. S. Caldarelli, M. Hong, L. Emsley, and A. Pines, *J. Phys. Chem.* **100,** 18696 (1996).
27. R. Challoner, R. K. Harris, and J. A. Tossell, *J. Magn. Reson.* **126,** 1 (1997).